J. of Thermal Science Vol.6, No.4

Local Convective Heat Transfer from Small Heaters to Impinging Submerged Axisymmetric Jets of Seven Coolants with Prandtl Number Ranging from 0.7 to 348

H. Sun C.F. Ma Y.Q. Tian

Department of Thermal Science & Engineering, Beijing Polytechnic University, Beijing 100022, China

Using seven working fluids, a systematic experimental study was performed to investigate the local convective heat transfer from vertical heaters to impinging circular submerged jets in the range of Reynolds number between 1.17×10^2 and 3.69×10^4 with the emphasis placed on the examination of Prandtl number dependence. Heat transfer coefficients at the stagnation point were collected and correlated with the plate held within and beyond the potential core. Radial distribution of the local heat transfer coefficient was measured with five test liquids. Based on the measured profiles of the local heat transfer, a correlation was developed to cover the entire range of the radial distance. Besides the present data, the correlations developed in this work were also compared with a large quantity of available data of circular air jets. General agreement was observed between the air data and the correlations.

Keywords: forced convection, jets, Prandtl number.

INTRODUCTION

Jet impingement has been extensively employed in technical processes to produce relatively high heat/mass fluxes. In comparison with the heat/mass transfer rates provided by conventional techniques with fluid flows parallel to the heat/mass transfer surface, a remarkable increase in transfer coefficients can be obtained in this fashion. In most cases air is used as the working medium. Examples of air jet applications include cooling of turbine blades and electronic components, annealing of metallic and plastic sheets, drying of textiles and paper, and tempering of glass. With liquid as the working fluid, impingement transfer coefficient can be increased several orders of magnitude in comparison with that of gas jets. Several liquids have been used in engineering, including oil jets in internal combustion engines[1], perfluorocarbon liquid and water jets in electronic devices[2,3], and water jets in hot rolling process of metals[4]. Much attention is being directed to the basic study of liquid jets recently[5-7].

For gas jets, rather good knowledge base has been available in open literature. Comprehensive reviews have been presented by Martin[8], Downs and James[9] and Jambunathan et al[10]. With regard to liquid jets, our investigation of heat transfer is still relatively incomplete. Consequently, it is naturally hoped to make extrapolation of the available extensive results for air jets to the cases of submerged liquid jets. However, careful examination should be made of the effect of Prandtl number on impingement heat transfer before the possible extrapolation, as the Prandtl number of liquid may be several orders higher than that of air. The Prandtl number dependence of impingement heat transfer can be expressed by power function of Prandtl number itself. The value of 0.42 was recommended by Martin[8] based on the comparison of mass transfer measurements[11] with the data of heat transfer to

Received October, 1997.

Nomenclature

A	area of heated surface
C	empirical constant
C_p	specific heat at constant pressure
d	jet nozzle diameter
h	local heat transfer coefficient
I	current intensity
k	thermal conductivity of fluid
l_p	potential core length
m, n	empirical constants
Nu	local Nusselt number, hd/k
P	empirical constant
Pr	Prandtl number, $Cp\mu$/k
q	heat flux, empirical constant
R	electrical resistance
r	radial distance from stagnation point, recovery factor
Re	Reynolds number, Ud/ν
T_{aw}	adiabatic wall temperature
T_j	jet static temperature at nozzle exit
T_w	wall temperature
U	mean fluid velocity at nozzle exit
z	nozzle–to–plate spacing
μ	dynamic viscosity
ν	kinematic viscosity

Subscripts

max	maximum value
0	stagnation point

air[8,12] and to water jets[13]. This value has been accepted extensively by many investigators to circular jets of air[14–17], water[2,5,7,18–21], R113[22,23] and perfluorocarbon[7,24]. However, power value of 1/3 was also adopted for circular jets of water[13,25–28], air[29–35], heavy electrochemical liquid[36,37] and fluorocarbon[27]. In order to investigate the effect of Prandtl number, Metzger et al.[38] employed both oil and water and Jiji and Dagan[27] used both water and FC-77 as working fluids in their experiments respectively. Metzger et al. suggested the exponent values of 0.24 and 0.487 for lubricating oil and water respectively. Value of 1/3 was determined experimentally for water and FC-77 by Jiji and Dagan. Besides the discrepancy in their results, it is also noted that both the two investigations[27,38] were related with averaged heat transfer of free–surface circular jets, not directly relevant to the present subject. Apparently, an accurate examination is still required for submerged axisymmetrical jets in a wide range of Prandtl number.

Research of impingement heat transfer was recently stimulated by the application in electronic equipment because of its excellent cooling performance[39]. On account of the sensitivity of the electronic performance on the thermal conditions, equipment designers need not only high heat transfer rate but also the uniformity of its distribution. Consequently, good knowledge base of local heat transfer with submerged liquid jets is required. Furthermore, in the geometric aspect the heat transfer process in electronic cooling is often characterized by small size and vertical orientation of the heat transfer surfaces.

The objective of this work is to carry out an extensive and consistent investigation to extend the experimental study of local heat transfer from small vertical heaters to single submerged circular jets of seven working fluids with Prandtl numbers ranging from 0.7 to 348. Measurements were made to supplement more data of the stagnation point and the radial distribution of heat transfer rates. The effects of jet velocity, nozzle-to-plate spacing and the thermal properties of working fluids were studied in experimental details. Emphasis was placed on examination of Prandtl number dependence of impingement heat transfer based on direct experimental comparison of the local heat transfer between various working mediums. Along with the preliminary results reported in Refs.[20,23,40,41], the expanded body of experimental result obtained in the present work provided a good data base for testifying the local impingement heat transfer performance and mechanism with working fluids from gas to large Prandtl numbers oil. Generalized correlations were developed for predicting local heat transfer with five groups of fluids: gas, water, freon, organic liquid and oil.

As the geometric arrangements in the present work designed for the request of electronic cooling, all the experimental data and correlations would be more valuable for the heat transfer engineers and equipment designers working in area of electronics.

EXPERIMENTAL APPARATUS AND METHOD

Experimental Apparatus

Seven fluids were chosen as the test mediums in this study, including air, nitrogen gas, water, R113, kerosene, ethylene glycol and transformer oil. The test fluid was circulated in a closed loop which had provi-

sion for filtering, metering, preheating and cooling as shown in Fig.1. The test chamber was constructed of stainless steel with three visual ports as illustrated in Fig.2. The bottom section of the cover on the chamber was transparent. A flexible polyethylene tube joined the two sections of the cover. The test section assembly was vertically fixed on the side of the chamber. The details of the test section assembly are presented in Fig.3. The main part was a strip of 10 μm thick constantan foil with a heated section of 5 mm × 5 mm (nominal) exposed to the coolant. The strip on either side of this active section was soldered to copper bus blocks, which were in turn connected to power leads. The heated section of the foil was cemented to a bakelite block inserted between the copper blocks. The assembly was cemented in a plexiglas disk fixed in a brass housing with a screwed flange. The test section was thermally highly insulated by fiberglass to minimize heat loss. The temperature of the center of the inner surface of the heater was measured with 40 gage iron-constantan thermocouple which was electrically insulated from the heater yet in close thermal contact. The active section of the constantan foil was used as an electrically heating element as well as a heat transfer surface. AC power to the test section was provided by a 50 A power supply.

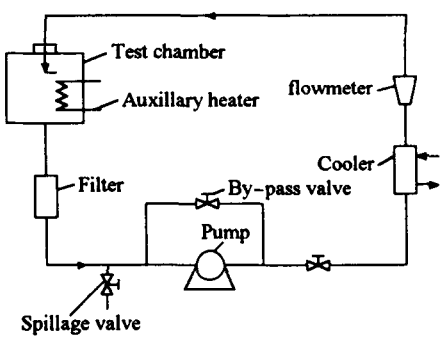

Fig.1 Schematic layout of flow loop

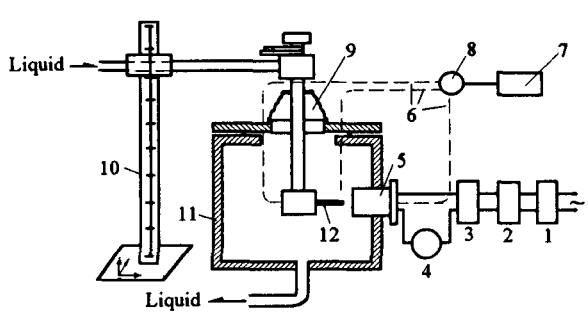

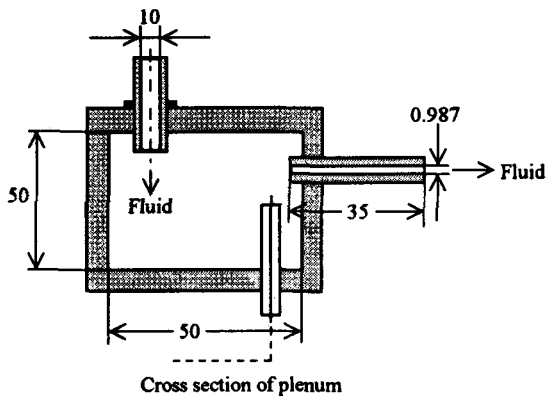

Fig.2 Details of test chamber and instrumentation

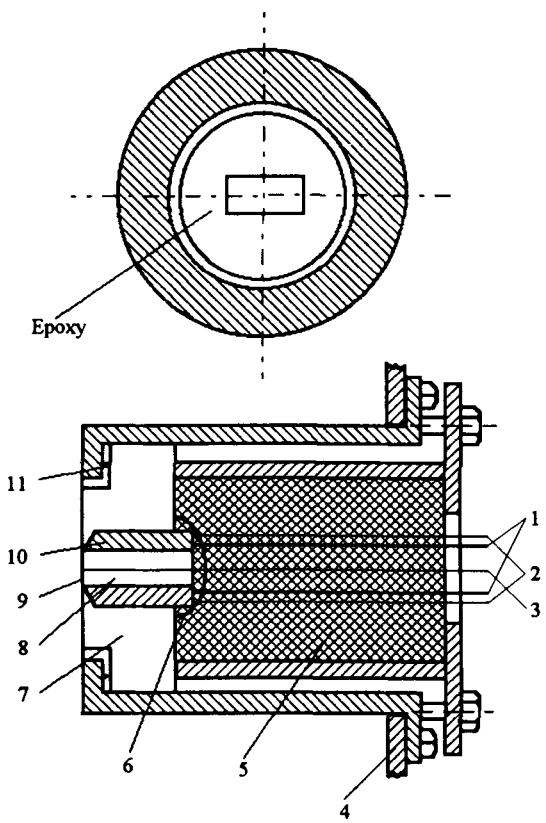

Fig.3 Details of electrically heated test section

The fluid jets issued from a horizontal jet tube of 0.987 mm inside diameter and 35 mm length. Using the large length-to-diameter ratio tube, a fully developed laminar pipe flow can be obtained at the nozzle exit. As shown in Fig.4 the fluid was supplied from a vertical delivery tube to the jet nozzle passing a plenum box. Their axes were perpendicular with each other in a vertical plane. The jet tube-delivery tube assembly was fixed on a three-dimensional coordinate rack and could be adjusted with respect to the test section with placements accomplished within

±0.01 mm. The jet temperature was measured with a 40 gage iron–constantan thermocouple placed inside the plenum box close to the entrance of the jet tube. The fluid temperature in the test chamber was also monitored by a thermocouple of the same type. Due to the flexible nature of the plastic seal at the top of the chamber, the pressure in the chamber is considered closed to the atmosphere.

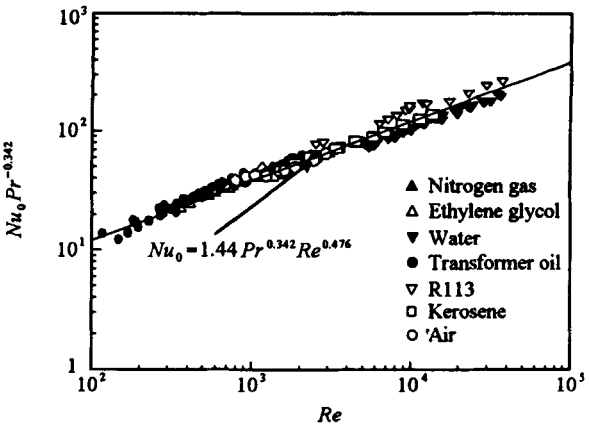

Fig.4 Heat transfer at stagnation point with the plate held within the potential core

Procedure and Data Reduction

The heat transfer surface was left in the original highly polished condition and cleaned with acetone before tests. The area of the heated surface was carefully measured for each test section with a tool maker's microscope of 0.001 mm resolution. Heat flux was calculated from the electrical power supplied to the test section and the area of one side of the heated surface. Heat flux was determined by the following formula:

$$q = I^2 R/A \tag{1}$$

where the resistance R was measured accurately with direct current before experiments. It was verified in preliminary tests that the variation of resistance with temperature could be neglected (less than ±0.1 percent), as the heater temperature variation was less than 40 K in the present study and the variation in resistance with temperature is extremely small for constantan. The current intensity was measured by an amperemeter.

In preliminary experiments the jet tube was oriented perpendicularly to the test section. The distance between the nozzle and the target surface was accurately adjusted by means of the three-dimensional frame. In order to ensure that the nozzle centerline coincided with the midpoint of the heater, a procedure of centering was developed whereby the jet was moved on the heated surface until minimum wall temperature was recorded by the thermocouple. The measured wall temperature at the heater center was taken as the local value. By recording this temperature for various locations of the jet tube the horizontal temperature distributions could be obtained for given jet conditions and surface heat flux. In the experiments the temperature of the jets and the fluid in the container were accommodated with each other so that their difference could be less than 1 K for eliminating the effect of ambient fluid entertainment into the impinging jets on the heat transfer process. The local heat transfer coefficient was calculated from the heat flux and the local wall temperature:

$$h = q/(T_w - T_{aw}) \tag{2}$$

where the adiabatic wall temperature was determined by

$$T_{aw} = T_j + r\frac{U^2}{2Cp} \tag{3}$$

where the velocity U was calculated from the measured flow rate and the nozzle area. The recovery factor "r" was obtained by the correlation recommended by some of the present author[33]:

$$r = Pr^{0.5} \tag{4}$$

The recovery factor effect was considered only with transformer oil as the test liquid. During the experiments, the difference between T_w and T_{aw} was adjusted to be maintained approximately at 10 K. Properties of the working fluid were evaluated at the film temperature by averaging the wall and jet temperatures.

In the present work, experiments were systematically performed with seven working fluids over wide ranges of experimental parameters as shown in Table 1.

Uncertainty of Experimental Results

The uncertainty in Nusselt number was influenced primarily by the determination of heat flux and wall temperature. The surface heat flux was affected by the variation of the constantan foil thickness that was claimed in the suppliers specification to be less than 3 percent of the normal value. This percentage value is taken as the indicator of heat flux variation due to foil thickness nonuniformity. Preliminary experiments were performed to check heat loss from the heater, and indicated that with jet impingement the maximum conduction loss to the back of the heater

Table 1 Experimental parameters in the present work

Fluid	Air	Nitrogen gas	water	R113	Kerosene	Ethylene glycol	Transformer oil
Re_d	8.01×10^2–2.91×10^4	(1.04-3.00) $\times 10^3$	5.22×10^3–3.63×10^4	2.52×10^3–3.69×10^4	1.49×10^3–2.36×10^3	3.55×10^2–2.06×10^3	1.17×10^2–
Pr	0.707–0.708	0.712–0.713	5.71–6.81	7.91–8.91	20.5–21.0	89.6–129	134–348

assembly was less than 0.8 percent of the power input to the heater. This conclusion was supported by a conduction analysis for this study. So, no correction was included for such conduction loss in this work. The determination of the heater surface temperature was related to the thermal resistance of the adhesive layer between the thermocouple lead and the back side of the foil. During the manufacture process the foil strip was strongly suppressed to the top surface of the bakelite block to minimize the thickness of the adhesive layer in between. Measurements were made of the adhesive thickness with several used test sections after their failure in experiments. The thickness was determined between 0.04 and 0.1 mm. Taking the typical value of the thermal conductivity of adhesive as 0.29 w/m·k, the thermal resistance across the adhesive layer was estimated between 1.38×10^{-4} and 3.45×10^{-4} k/w. As the conduction heat loss was less than 0.8% of the power input, and its main part passed through the bars, the uncertainty arising from positioning of the thermocouple lead was estimated to be always less than 0.28 K in this study. Another source of the uncertainty in wall temperature was concerned with lateral heat conduction along the constantan foil caused by the sharp radial variation of the heat transfer coefficient around the stagnation zone. Using the measured wall temperature distribution, this uncertainty was determined to be negligible (less than 0.8%) due to the extremely small thickness of the foil. All the thermocouple were calibrated to an accuracy of ±0.1 k before experiments. The uncertainty in Nusselt number was determined to be less than ±5 percent. The uncertainty in Reynolds number was affected by the measurement of the flow rate and the nozzle exit area. While the flowmeter was carefully calibrated, the nozzle exit area was precisely determined using the tool maker's microscope of 0.001 resolution. The uncertainty in Reynolds number did not exceed ±5.5 percent.

EXPERIMENTAL RESULTS AND DISCUSSION

Heat Transfer at Stagnation Point

Heat transfer at stagnation point was first examined with the target surface held within the potential core. Based on the measurements of local wall temperature and heat flux, the heat transfer coefficients at stagnation point were obtained with the seven fluids in the range of Prandtl and Reynolds numbers listed in Table 1. A total of 169 experimental points were collected and correlated, including 12 air points, 7 nitrogen gas points, 46 water points, 14 R113 points, 19 kerosene points, 25 ethylene glycol points and 46 transformer oil points. An attempt was made to develop a generalized correlation that can be used for all the data with the seven test fluids. It has been well established both by analytical[8,10,28,42,43] and experimental[5,10,19,20,23,40,41] investigations that the stagnation point Nusselt number can be described quite well by a power-law dependence on Reynolds and Prandtl number

$$Nu_0 = CPr^m Re^n \tag{5}$$

where the constant C depends on jet turbulence intensity and mean radial velocity gradient[6]. Actually, it has been determined from experimental investigations[44–47] that the local heat transfer at stagnation zone was much more sensitive to the flow field characteristics than that in wall jet zone. It has been reported for fluid jets that differences in the constant C up to 40 percent may be caused by the changes in the turbulence intensity[44–47] or the velocity gradient[44]. A multivariate least-squares curve fit was performed to determine the coefficients C, m, and n in Eq.(5), presenting the result: C=1.44, m=0.342, and n=0.476. With this set of constants, the average error and the mean deviation of all the experimental data from Eq.(5) are ±8.2 and 10.7 percent, respectively. For all the 169 data points of the seven fluids, Eq.(5) with these empirical constants presents 91.4 percent of the data within ±20%. Fig.4 illustrates a comparison between the prediction and the experimental data. Good agreement is seen from the figure. It is noted that the exponent of Reynolds number 0.476 determined here is very close to 0.5 that has been verified both by available analytical solutions[10,28,42,43] and the experimental studies[5,6,8,9,20,23,40,44]. This value demonstrates the

laminar characteristics of the flow within the stagnation zone, in which favorable pressure gradient parallel to the target surface tends to laminarize the fluid flow. Adopting this Reynolds number dependence, attention was focused on determination of the dependence of stagnation point Nusselt number on Prandtl number. An analytical study[43] for free-surface round jets revealed the Prandtl number dependence that m=0.4 for $Pr < 3$, m=0.37 for $3 < Pr < 10$, and $m = 1/3$ for $Pr > 10$. It may be postulated that this result can be used for submerged jets at the stagnation point. Exponent of 0.4 has been widely accepted for gas[8,12,14-17], water[7,8,18-21], freon[22,23] and fluorocarbon[7] with Prandtl number less than 20. In the case of Prandtl number higher than 20, power value of 1/3 was used for transformer oil and ethylene glycol[41] and heavy electrochemical liquid[36,37]. Taking into account the above, it seems reasonable to have two different values of the power of Prandtl number for larger and smaller Prandtl numbers respectively. After thoroughly checking the Prandtl number dependence with the present experimental results of the seven working fluids, it is proposed that the exponent value may be set equal to 0.4 for gas and 1/3 for liquid respectively. With m=0.4 or 1/3, and n=1/2, the coefficient C in Eq.(5) was determined using a least-squares technique to be 1.21 that is very close to 1.29 obtained in Refs.[20,22,23,,40,41]. With this set of constants the generalized correlation represents 85 percent of the experimental data of seven fluids within ±17 percent with an average error and a mean absolute deviation equal to ±9.93 and 11.9 percent of all the experimental data, respectively. The accuracy of this correlation is almost equal to that presented in Fig.4. As shown in Fig.5, this Prandtl and Reynolds number dependence is strongly supported by the present experimental data. Eq.(5) is fairly successful at collapsing all the liquid data with m=1/3 for liquid. But it would fail to collapse the data for large Prandtl number liquid if a single value of 0.4 is taken for all the fluids. With m=0.4 the correlation lies significantly above the data at higher Prandtl number as shown in Fig.5.

The foregoing discussion is concerned only with small nozzle-to-plate spacing. In the present work, the variation of the stagnation point heat transfer with the spacing was also measured and examined using the five test liquids. The experimental results are presented in Fig.6. Actually, immediately upon leaving the nozzle, the jet begins to enter the surrounding still fluid, but up to some points (the end of the so-called potential core), the jet velocity at the center-lines is unaffected by the mixing and remains equal to the velocity at nozzle exit. Inside the potential core the jet velocity essentially keeps constant. For higher

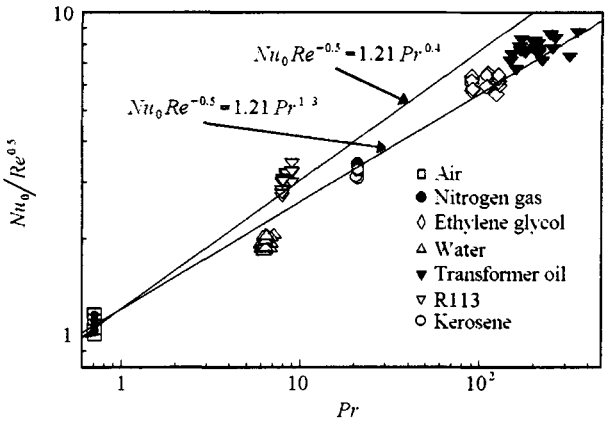

Fig.5 Prandtl number dependence of stagnation point heat transfer

Reynolds number, the heat transfer coefficient maybe progressively increases with the nozzle-to-plate spacing and reaches its peak at the end of potential core, as observed with water jets in Fig.6(a). It is seen from the figure that with jet Reynolds number around 2×10^4 the variation of Nusselt number was over 10 percent inside the potential core. This increase can be attributed to the enhancement by the turbulence generated by jet itself. For lower Reynolds number the variation of heat transfer coefficient is slight inside the potential core as shown in Fig.6 with the other test liquids. Beyond the potential core, the arrival velocity begins to decline significantly, being inversely proportional to the spacing. Consequently, according to Eq.(5), the heat transfer coefficient is inversely proportional to the square root of the spacing. After normalization by the maximum Nusselt number at the tip of the potential core, the stagnation point heat transfer coefficients beyond the potential core can be expressed by:

$$\frac{Nu_0}{Nu_{0,\max}} = \left(\frac{l_p/d}{Z/d}\right)^{1/2} \tag{6}$$

where l_p/d is the nondimensional length of the potential core. It was found that l_p/d was nearly a constant for each test liquid in the range of the present experimental study. The approximate values of l_p/d was determined from the experimental data that $l_p/d = 8$ for transformer oil and ethylene glycol with $Re_d < 10^3$, and $l_p/d = 5$ for water, kerosene and R113 in the range of $Re_d = 3.7 \times 10^3 - 2.9 \times 10^4$. Apparently, the mixing of the jet flow with surrounding fluid is intensified by increasing of the Reynolds number, resulting in the shortening of potential core. Good agreement

is seen from Fig.6 between the correlation and the experimental data with the five test liquids. The inverse proportion of stagnation point heat transfer with the nozzle–to–plate spacing was also reported by Rao and Trass[48] for submerged circular water jets. Using a mass transfer technique they experimentally determined the exponent in Eq.(6) as 0.54 which is almost identical with the value of 1/2 proposed in the present work.

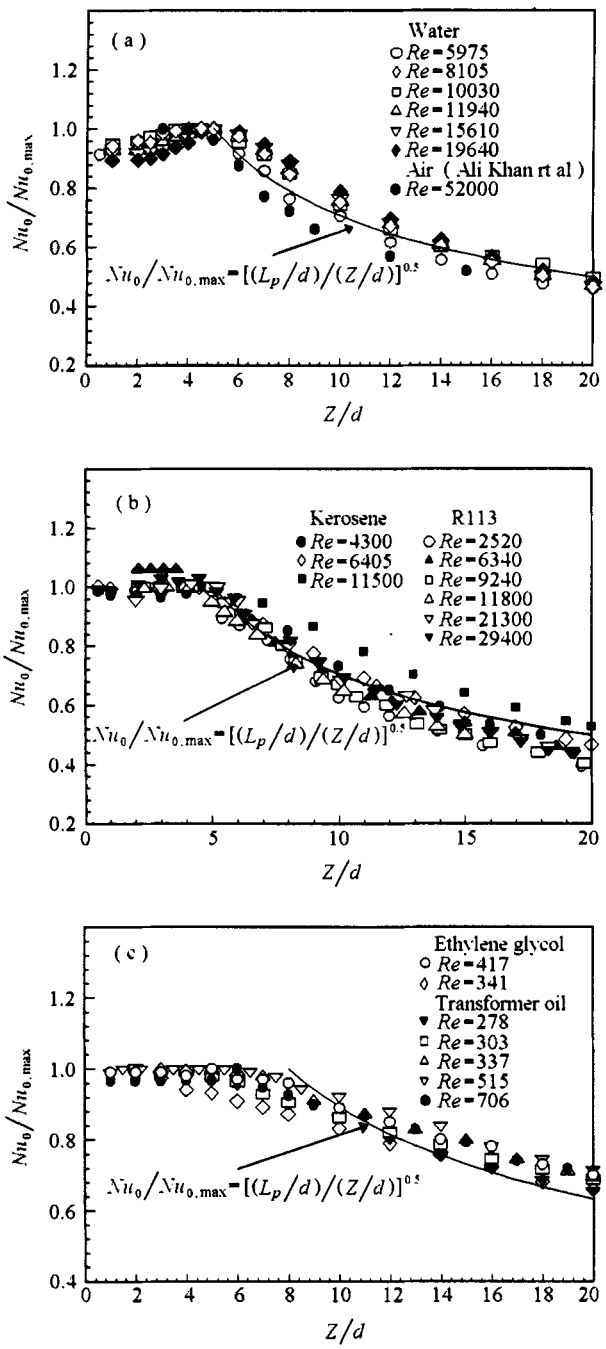

Fig.6 Effect of nozzle–to–plae spacing on stagnation point heat transfer
(a) water and air (b) kerosene and R113
(c) ethylene glycol and transformer oil

Radial Distribution of Local Heat Transfer Coefficient

Measurements were made to determine the radial variation of local heat transfer coefficient with the target located within the potential core for water, R113, kerosene, ethylene glycol, and transformer oil. The results are presented in nondimensional form by the Nusselt number in Fig.7, including 26 radial profiles and 475 data points. As shown in the figures the distribution curves are characterized by bell shape with maximum at stagnation point. Since the local heat transfer coefficient distribution curves are symmetrical about the stagnation point, only half profiles are plotted in Fig.7. After normalization of the local values by the maxima at the stagnation point, all the distribution curves seem to collapse to a single profile as shown in the figures. In first approximation, Nu/Nu_0 can be considered as a function of radial distance from the stagnation point, nearly independent of Reynolds number and Prandtl number. An attempt was made to correlate all the data of radial distribution by a generalized formula for the five test liquids. The flow field of circular jet impingement on a flat plate may be subdivided into two characteristic regions: the stagnation zone and wall jet zone[6–8]. In the stagnation zone ($r/d < 2$), it is seen from the figures that the normalized Nusselt number seems essentially independent of Reynolds number. Based on a semi–empirical model, a correlation was presented by Ma and Bergles[23]:

$$\frac{Nu}{Nu_0} = (r/d)^{-0.5}\tanh^{0.5}(0.88r/d) \quad \text{for} \quad 2 > \frac{r}{d} > 0 \tag{7}$$

Eq.(7) was modified to correlate all the data of the five liquids collected in this work:

$$\frac{Nu}{Nu_0} = \left[\frac{\tanh(1.137r/d)}{r/d}\right]^{0.999} \quad \text{for} \quad 2 > \frac{r}{d} > 0 \tag{8}$$

This correlation is within ±20 percent of 73% data points with an average error of ±14.5 percent for all the data of the five liquids.

For wall jet zone ($r/d > 2$), an empirical correlation was proposed[23]:

$$\frac{Nu}{Nu_0} = P(r/d)^{-q} \tag{9}$$

where the constants P and q were determined experimentally. For R113, transformer oil and ethylene glycol, it was suggested that $P = 1.49$ and $q = 1.25$ by Ma and Bergles[23] and Ma et al.[41]. Sun et al.[20] obtained $P = 1.69$ and $q = 1.07$ for water jets. In order to get a general correlation for all the liquid and air

jets investigated in this work, the experimental data were examined together. Values of $P = 1.011$ and $q = 0.867$ were chosen from a least-squares analysis to minimize the standard deviation of the data with various fluids in the present study.

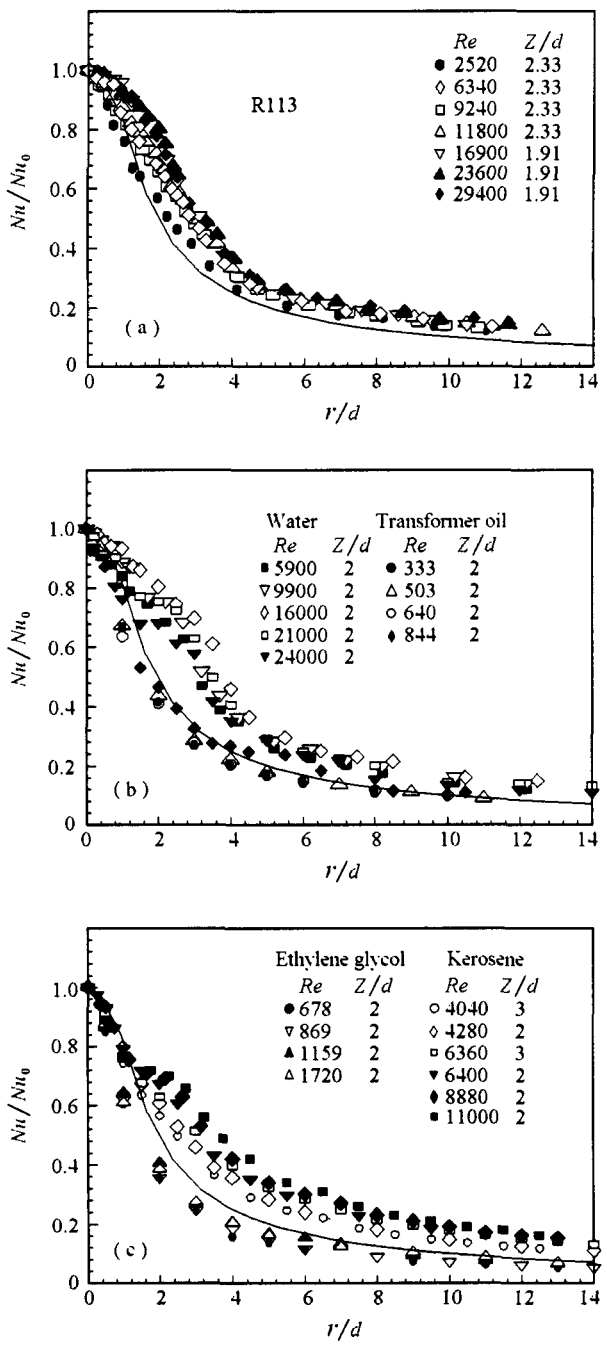

Fig.7 Radial distribution of local heat transfer coefficients with the targets with the potential core
(a) (R113)
(b) water and transformer oil
(c) ethylene glycol and kerosene

It is convenient to have a general expression that covers the entire range of radial distance ($r/d < 14$). Based on the correlation technique presented by Churchill and Usagi[49], a generalized correlation was developed:

$$\frac{Nu}{Nu_0} = \left\{\left[\frac{\tanh(1.137r/d)}{r/d}\right]^{0.999} + \left[1.011(r/d)^{-0.867}\right]^n\right\}^{1/n}$$

$$\text{for} \quad 0 < \frac{r}{d} < 14 \qquad (10)$$

It was found that the accuracy of Eq.(10) with $n = -17$ is high enough. Correlation curve of Eq.(10) with $n = -17$ is presented in Fig.7. The correlation is within $\pm 35\%$ of 82% of the experimental data. The average error of the correlation is ± 23.2 percent for all the data of the five liquids in both stagnation and wall jet zones ($0 < r/d < 8$). In first approximation, Eq.(10) can be used to estimate the radial variation of local heat transfer for the liquid jets in a wide range of $Re = 333 - 294000$, and $Pr = 5.7 - 348$.

Examination of the water data for $Re = 20600$ presented in Fig.7(b) indicates the presence of a hump appearing in the profile at about $r/d = 1.9$. For lower Reynolds numbers similar but less changes in the slope of $Nu/Nu_0 \sim r/d$ curves are observed in the same location both with water and kerosene data in Fig.7(b) and (c), respectively. This phenomenon was also reported for circular free-surface water jets by Stevens and Webb[19], and for circular air jets by Gardon and Akfirat[46], Obot et al.[45], Hrycak[54], Gundappa et al.[55], Baughn and Shinizu[58], and Chia et al.[56]. It was attributed by the investigators to transition from laminar to turbulent flow. It is noted that the locations of the peaks or the sharp knees in the profiles are essentially identical between the liquid and air jets. Inflection of transition to turbulence was not taken into account in the correlation of the radial local heat transfer profiles. This factor is certainly responsible, at least partially, for the scatter of the high Reynolds number experimental data in the vicinity of $r/d = 1.9$.

Measurements were also made with the targets placed beyond the potential core. The typical result with R113 is presented in Fig.8. As shown in the figure, the bell-shape profiles become flatter with the increasing of nozzle-to-plate spacing. It is also seen from the figure, that the maximum heat transfer coefficient at the stagnation point decreases with increasing of the spacing as described in Eq.(6).

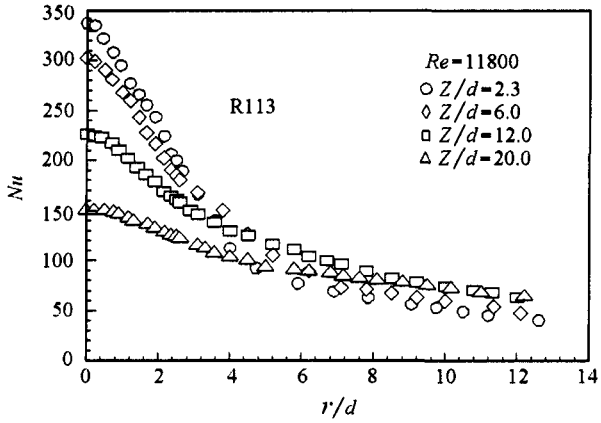

Fig.8 Heat transfer profiles with the plate beyond the potential core

Comparison with Circular Air Jet Data

One of the main objectives of this work is to check the similarity and difference between air and liquid jets. In this study, the main body of experimental data was related to liquids, only limited data points were collected with air and nitrogen gas. An attempt was made to make comparison of the present results with circular air jet data from other resources. A total of more than 105 data points were quoted from 17 references for the comparison. Based on the comparison it is hoped to extrapolate the knowledge base of air jets to the cases of liquid jets. The key issue of this extrapolation is the effect of Prandtl number on impingement heat transfer. Fig.9 demonstrates the comparison of predicted curve by Eq.(5) with the air jet data from 17 references. A general agreement between the data and the correlation is seen from the figure. The average error is ±11.4 percent, and the standard deviation is 13.8 percent. Considering the sensitivity of the heat transfer at stagnation zone, where the flow is in laminar regime, and the difference in the experimental conditions and experimental methods of the investigations, the agreement should be satisfied. Fig.9 indicates the fact that the correlation developed in this work can be also used for predicting the stagnation point heat transfer with circular air jets. The validity of Eq.(6), which describes the variation of stagnation point heat transfer with nozzle-to-plate spacing, for air jet was also checked with the data by Ali Khan et al.[59]. As shown in Fig.6(a), the experimental data of air jets agree well with the correlation. Finally, comparison is made of local heat transfer profiles between liquid and air jet at same nozzle-to-plate spacing. In Fig.10, the experimental data of kerosene and R113 are plotted along with air jets data from four references[12,50,52,60]. It is seen from the figure that the profiles of the two liquids are similar with the air jet profiles. The comparisons illustrated in Figs.6,9,10 indicate the similarity of local heat transfer performance between liquid and air jets. This result laid a base of extrapolating the air jet knowledge to the case of liquid jets.

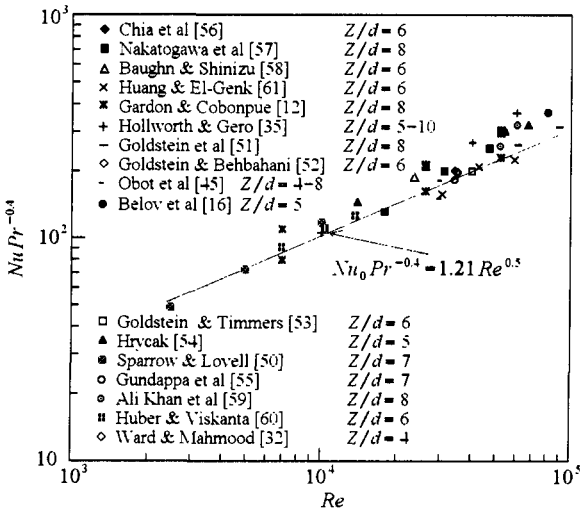

Fig.9 Comparison of Eq.(5) with circular air jet data

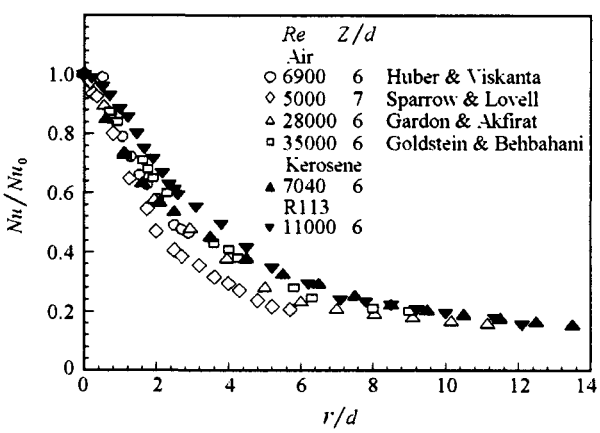

Fig.10 Comparison of radial profiles of local heat transfer between liquid jet data and circular air jet data

CONCLUSIONS

1. Local characteristics of the convective heat transfer from small vertical heaters to single impinging circular submerged jets of seven working fluids in the range of $Re = 1.17 \times 10^2 \sim 369 \times 10^4$ are experimentally studied with emphasis placed on the examination of Prandtl number dependence.

2. Heat transfer coefficient at the stagnation point with the targets held within potential core can be well

correlated by Eq.(5) for all the seven coolants. The influence of the nozzle–to–plate spacing can be predicted by Eq.(6).

3. Radial distribution of the local heat transfer with the targets placed within the potential core can be approximately correlated by Eq.(10) in the entire region of radial distance. Beyond the potential core, the profiles became flatter with the increasing of the spacing.

4. The Eqs.(5),(6), and (10) were compared with the experimental data of circular air jets from other resources. General agreements were observed, demonstrating the validity of the correlations developed in the present work both for circular liquid and gas jets.

Acknowledgment

This work was supported by the National Natural Science Foundation of China. The authors also express their thanks to Profs. D.H. Lei and Y.P. Gan and Mr. Y. Zhuang for the assistance in experimental work.

REFERENCES

[1] Kiryu, M., "Development of Oil–Cooled 750cc Motorcycle Engine," Automobile Technology (in Japanese), **40,** pp.1154–1158, (1986).

[2] Yamamoto, H., Udagawa, Y., and Suzuki, M., "Cooling system for FACOM M–780 Large–Scale Computer," Cooling Technology for Electronic Equipment, W. Aung, ed., Hemisphere Publishing Corporation, pp.701–714, (1987).

[3] Wadsworth, D.C. and Mudawar, I., "Cooling of Multichip Electronic Module by Means of Confined Two–Dimensional Jets of Dielectric Liquid," *ASME J. Heat Transfer,* **112,** pp.891–898, (1990).

[4] Kohing, F.C., "Waterwall: Water Cooling System," Iron–Steel Engineer, **62,** pp.30–36, (1985).

[5] Faggiani, S., and Grassi, W., "Impinging Liquid Jets on Heated Surfaces," Proceedings of the Ninth International Heat Transfer Conference, **1,** pp.275–285, (1990).

[6] Webb, B.W., and Ma, C.F., "Single–Phase Liquid Jet Impingement Heat Transfer," Advances in Heat Transfer, **26,** pp.105–217, (1995).

[7] Womac, D.J., Ramadhyani, S., and Incropera, F.P., "Correlating Equations for Impingement Cooling of Small Heater Surfaces with Single Circular Liquid Jets," *ASME J. Heat Transfer,* **115,** pp.106–115, (1993).

[8] Martin, H., "Heat and Mass Transfer between Impinging Gas Jets and Solid Surfaces," Advances in Heat Transfer, **13,** pp.1–60, (1977).

[9] Downs, S.J., and James, E.H., "Jet Impingement Heat Transfer–A Literature Survey," ASME Paper 87–HT–35, (1987).

[10] Jambunathan, K., Lai, E., Moss, M.A., and Button, B.L., "A Review of Heat Transfer Data for Single Circular Jet Impingement," *Int. J. Heat and Fluid Flow,* **13,** No.2, pp.106–115, (1992).

[11] Schlunder, E.U. and Gnielinski, V., "Warme–und Stoffubertragung zwischen gut und aufprallendem Dusenstrahl," *Chem. Ing. Tech.,* **39,** pp.578–584, (1967).

[12] Gardon, R., and Cobonpue, J., "Heat Transfer between a Flat Plate and Jets of Air Impinging on it," International Developments in Heat Transfer, pp.454–460, ASME, New York, (1962).

[13] Smirnov, V.A., Verevochkin, G.E., and Brdlick, P.M., "Heat Transfer between a Jet Held Plate Normal to Flow," *Int. J. of Heat and Mass Transfer,* **2,** pp.1-7, (1961).

[14] Nakatogawa, T., Nishiwaki, N., Hirata, M., and Torii, K., "Heat Transfer of Round Turbulent Jet Impinging Normally on Flat Plate," Proceedings of the Fourth International Heat Transfer Conference, **2,** FC 5.2, (1970).

[15] Hrycak, P., "Heat Transfer from Impinging Jets to a Flat Plate," *Int. J. of Heat and Mass Transfer,* **26,** pp.1857–1865, (1983).

[16] Belov, I.A., Gorshkov, G.F., Komarov, V.S., and Terpigoryev, V.S., "Experimental Study of Heat Transfer in a Subsonic Jet Impinging Normally on a Plate Baffle," Heat Transfer–Soviet Research, **4,** No.4, pp.17–20, (1972).

[17] Krotzsch, P., "Warme–und Stoffubergang bei prallstromung aus Dusen und Blendenfeldern," *Chem. Ing. Tech.,* **40,** pp.339–344, (1968).

[18] Kiper, A.M., "Impinging Water Jet Cooling of VLST Circuits," Int. Comm. Heat and Mass Transfer, **11,** pp.517–526, (1984).

[19] Stevens, J., and Webb, B.W., "Local Heat Transfer Coefficients under an Axisymmetric, Single–Phase Liquid Jet," *ASME J. of Heat Transfer,* **113,** pp.71–78, (1991).

[20] Sun, H., Ma, C.F., and Nakayama, W., "Local Characteristics of Convective Heat Transfer from Simulated Mircroelectronic Chips to Impinging Submerged Round Water Jets," *ASME J. Electronic Packaging,* **115,** pp.71–77, (1993).

[21] Elison, B., and Webb, B.W., "Local Heat Transfer to Impinging Liquid Jets in the Initially Laminar, Transitional and Turbulent Regimes," *Int. J. of Heat and Mass Transfer,* **37,** No.8, pp.1207–1216, (1994).

[22] Ma, C.F., and Bergles, A.E., "Boiling Jet Impingement Cooling of Simulated Microelectronic Chips," ASME HTD–**28,** pp.5-12, (1983).

[23] Ma, C.F., and Bergles, A.E., "Convective Heat Transfer on a Small Vertical Heated Surface in an Impinging circular Liquid Jet," In Heat Transfer Science and Technology 1988, Edited by Wang, B.X., Hemisphere, pp.193–200, (1990).

[24] Maddox, D.E., and Bar–Cohen, A., "Thermofluid Design of Submerged Jet Impingement Cooling for Electronic Components," ASME HTD–**171,** Heat Transfer in electronic Equipment, pp.71–80, (1991).

[25] Sitharamayya, S., and Subba Raju, K., "Heat Transfer between an Axisymmetric Jet and a Plate Held Normal to the Flow," *Canadian J. Chem. Eng.*, **47**, pp.365–368, (1969).

[26] Yonehara, N., and Ito, I., "Cooling Characteristics of Impinging Multiple Water Jets on a Horizontal Plate," Tech. Report, Kansai University, No.20, (1983).

[27] Jiji, L.M., and Dagan, Z., "Experimental Investigation of Single Phase Multi–Jet Impingement Cooling of an Array of Microelectronic Heat Sources," Cooling Technology for Electronic Equipment, Edited by Win Aung, Hemisphere, pp.332–352, (1988).

[28] Liu, X., Lienhard, J. H., and Lombara, J.S., "Convective Heat Transfer by Impingement of Circular Liquid Jets," *ASME J. of Heat Transfer,* **113**, pp.571–582, (1991).

[29] Perry, K.P., "Heat Transfer by Convection from a Hot Gas Jet to a Plane Surface," Proceedings of the Inst. Mech. Eng., **168**, pp.775–780, (1954).

[30] Florschuetz, L.W., Truman, C.R., and Metzger, D.E., "Streamwise flow and Heat Transfer Distributions for Jet Array Impingement with Crossflow," ASME paper, 81–GT–77, (1981).

[31] Beltaos, S., "Oblique Impingement of Circular Turbulent Jets," *J. Hydraulic Research,* **14**, pp.17–36, (1976).

[32] Ward, J., and Mahmood, H., "Heat Transfer from a Turbulent, Swirling, Impinging Jet," Proceedings of 7th Int. Heat Transfer Conference, pp.401–408, (1982).

[33] Kercher, D.M., and Tabakoff, W., "Heat Transfer bvy a Square Array of Round Air Jets Impinging Perpendicular to a Flat Surface Including the Effect of Spent Air," ASME Paper, 69–GT–4, (1969).

[34] Huang, G.C., "Investigations of Heat Transfer Coefficients for Air Flow Through Round Jets Impinging Normal to a Heat Transfer Surface," *ASME J. of Heat Transfer,* **85**, pp.237–243, (1963).

[35] Hollworth, B.R., and Gero, L.R., "Entrainment Effects on Impingement Heat Transfer: Part II–Local Heat Transfer Measurements," *ASME J. Heat Transfer,* **107**, pp.910–915, (1985).

[36] Nakoryakov, V.E., Pokusaev, B.G., and Troyan, E.N., "Impingement of an Axisymmetric Liquid Jet on a Barrier," *Int. J. of Heat and Mass Transfer,* **21**, pp.175–184, (1978).

[37] Nataoka, K., and Mizushina, T., "Local Enhancement of the Rate of Heat Transfer in an Impinging Round Jet by Free Stream Turbulence," Heat Transfer–1974, **2**, pp.305–309, (1974).

[38] Metzger, D.E., Cummings, K.N., and Ruby, W.A., "Effects of Prandtl Number on Heat Transfer Characteristics of Impinging Liquid Jets," Proceedings of 5th International Heat Transfer Conference, Hemisphere, **2**, pp.20–24, (1974).

[39] Bar–Cohen, A., "Thermal Management of Electronic Components with Dielectric Liquids," *JSME Int. J. Series B.,* **36**, No.1, pp.1–23, (1993).

[40] Ma, C.F., Tian, Y.Q., Sun, H., Lei, D.H., and Bergles, A.E., "Local Characteristics of Heat Transfer from a Small Heater to an Impinging Round Jet of Liquid of Large Prandtl Number," in Heat Transfer Enhancement and Energy Conservation, Edited by Deng S.J., Hemisphere, pp. 305–309, (1974).

[41] Ma, C.F., Sun, H., Auracher, H., and Gomi, T., "Local Convective Heat Transfer from Vertical Heated Surfaces to Impinging Circular Jets of Large Prandtl Number Liquid," Proceedings of the Ninth Int. Heat Transfer Conf., **2**, pp.441–446, (1990).

[42] Wang, X.S., Dagan, Z., and Jiji, L.M., "Heat Transfer between a Circular Free Impinging Jet and a Solid Surface with Nonuniform Wall Temperature or Wall Heat Flux–Solution for the Stagnation Region," *Int. J. of Heat and Mass Transfer,* **32**, No.7, pp.1351–1360, (1989).

[43] Ma, C.F., Zhao, H.Y., Masuoka, T. and Gomi, T., "Analytical Study on Impingement Heat Transfer with Single Phase Free–Surface Circular Liquid Jets under Arbitrary Heat Flux Condition," *Journal of Thermal Science,* **5**(4), pp.271–277, (1996).

[44] Pan, Y., Stevens, J., and Webb. B.W., "Effect of Nozzle Configuration on Transport in the Stagnation Zone of Axisymmetric, Impinging Free–Surface Liquid Jets: Part 2–Local Heat Transfer," *ASME J. Heat Transfer,* **114**, pp.880–885, (1992).

[45] Obot, N.T., Majumdar, A.S., and Douglas, W.J.M., "The Effect of Nozzle Geometry on Impingement Heat Transfer Under a Round Turbulent Jet," ASME Paper 79–WA/HT–53, (1979).

[46] Gardon, R., and Akfirat, J.C., "The Role of Turbulence in Determination the Heat Transfer Characteristics of Impinging Jets," *Int. J. of Heat and Mass Transfer,* **8**, p.1261–1272, (1965).

[47] Hoogendoorn, C.J., "The Effect of Turbulence on Heat Transfer at a Stagnation Point," *Int. J. of Heat and Mass Transfer,* **20**, pp.1333–1338, (1977).

[48] Rao, V.V., and Trass, O., "Mass Transfer from a Flat Surface to an Impinging Turbulent Jet," *Canadian J. Chem. Eng.,* **42**, No.3, pp.95–99, (1964).

[49] Churchill, S.W., and Vsagi, R., "A General Expression for the Correlation of Rates of Transfer and other Phenomena," *AIChE J.,* **18**, pp.1121–1128, (1972).

[50] Sparrow, E., and Lovell, B.J., "Heat Transfer Characteristics of an Obliquely Impinging Circular Jet," *ASME J. Heat Transfer,* **102**, pp.202–207, (1980).

[51] Goldstein, R.J., Behbahani, A.I., and Heppelmann, K.K., "Streamwise Distribution of the Recovery Factor and the Local Heat Transfer Coefficient to an Impinging Circular air Jet," *Int. J. of Heat and Mass Transfer,* **29**, pp.1227–1382, (1986).

[52] Goldstein, R.J., Behbahani, A.I., "Impingement of Circular Jet With and Without Cross Flow," *Int. J. of Heat and Mass Transfer,* **25**, 1377–1382, (1982).

[53] Goldstein, R.J., and Timmers, J.F., "Visualization of Heat Transfer from Array of Impinging Jets," *Int. J. of Heat and Mass Transfer,* **25**, pp.1857–1868, (1982).

[54] Hrycak, P., "Heat Transfer from Impinging Jets to a Flat Plate with Conical and Ring Protuberances," *Int. J. of Heat and Mass Transfer,* **27**, pp.2145–2154, (1984).

[55] Gundappa, M., Hudson, J.F., and Diller, T.E., "Jet Impingement Heat Transfer from Jet Tubes and Orifices," ASME HTD-**107,** pp.43–50, (1989).

[56] Chia, C.J., Ciralt, F., and Trass, O., "Mass Transfer in Axisymmetric Turbulent Impinging Jets," *Int. Eng. Chem., Fund.,* **16,** pp.28–35, (1977).

[57] Nakatogawa, T., Nishiwati, N., Hirata, M., and Torii, K., "Heat Transfer of Round Turbulent Jet Impinging Normally on Flat Plate," Heat Transfer–1970, **2,** FC 5.2, (1970).

[58] Baughn, J.W., and Shinizu, S., "Heat Transfer Measurement from a Surface with Uniform Heat Flux and an Impinging Jet," *ASME J. of Heat Transfer,* **111,** pp.1096–1098, (1989).

[59] Ali Khan, M.M., Sagi, N., Hirata, M., and Nishiwaki, N., "Heat Transfer Augmentation in an Axisymmetric Impinging Jet," Heat Transfer–1982, **3,** pp.363–368, (1982).

[60] Huber, A.M., and Viskanta, R., "Effect of Jet – Jet Spacing on Convective Heat Transfer to Confined Impinging Arrays of Axisymmetric Air Jets," *Int. J. of Heat and Mass Transfer,* **37,** pp.2859–2969, (1994).

[61] Huang, L., and El–Genk, M.S., "Heat Transfer of an Impinging Jet on a Flat Surface," *Int. J. of Heat and Mass Transfer,* **37,** No.13, pp.1915–1923, (1994).